Available online at www.sciencedirect.com

ScienceDirect

journal homepage: www.elsevier.com/locate/he

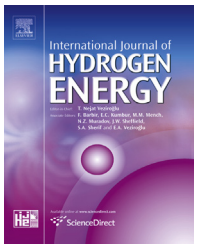

Controlled mechanochemical synthesis and hydrogen desorption mechanisms of nanostructured Mg_2CoH_5

G. Zepon [a,*], D.R. Leiva [b], M.J. Kaufman [c], S.J.A. Figueroa [d], R. Floriano [e], D.G. Lamas [f], A.A.C. Asselli [b], W.J. Botta [b]

[a] Programa de Pós-graduação em Ciência e Engenharia de Materiais, Universidade Federal de São Carlos, Rodovia Washington Luiz, km 325, CEP 13565-905, São Carlos, SP, Brazil

[b] Departamento de Engenharia de Materiais, Universidade Federal de São Carlos, Rodovia Washington Luiz, km 325, CEP 13565-905, São Carlos, SP, Brazil

[c] Department of Metallurgical and Materials Engineering, Colorado School of Mines, 1500 Illinois Street, Golden, CO, USA

[d] Laboratório Nacional de Luz Síncrotron, Centro Nacional de Pesquisa em Energia e Materiais Rua Giuseppe Máximo Scolfaro, 10000, Caixa Postal 6192, CEP 13083-970, Campinas, SP, Brazil

[e] Faculdade de Ciências Aplicadas, Universidade Estadual de Campinas, Rua Pedro Zaccaria, 1300, CEP 13484-350, Limeira, SP, Brazil

[f] CONICET and UNSAM, Escuela de Ciencia y Tecnología, 25 de Mayo y Francia, C.P.: 1650, San Martín, Buenos Aires, Argentina

ARTICLE INFO

Article history:
Received 12 September 2014
Received in revised form
9 November 2014
Accepted 15 November 2014
Available online 10 December 2014

Keywords:
Reactive milling
Mg-based complex hydride
Mg_2CoH_5
In-situ XRD
Desorption mechanisms

ABSTRACT

Magnesium complex hydrides are attractive for hydrogen storage applications, mainly due to their high volumetric capacities and to their relatively low cost. In this work, nanocrystalline Mg_2CoH_5 was synthesized with very high yields (97%) by reactive milling cobalt and magnesium under relatively mild processing conditions (30 bar of H_2 pressure and 12 h of milling). The behavior of the milled Mg_2CoH_5 during heating was studied by a combination of several techniques including DSC, QMS, TGA and in-situ synchrotron XRD. It is shown for the first time that two different mechanisms of hydrogen desorption take place. At low temperatures (up to 325 °C), some hydrogen is released by a diffusional mechanism with no change in the crystalline structure of the high temperature γ-Mg_2CoH_5 phase. At higher temperatures, above 325 °C, the γ-Mg_2CoH_5 phase becomes unstable and the complex hydride decomposes into Mg, Co and H_2. This is the first work to report the diffusional hydrogen desorption mechanism for the Mg_2CoH_5 or any other complex hydride. Furthermore, a complete description of the allotropic β-Mg_2CoH_5 to γ-Mg_2CoH_5 phase transition is provided.

* *Corresponding author.*
E-mail address: guizepon@yahoo.com.br (G. Zepon).
http://dx.doi.org/10.1016/j.ijhydene.2014.11.085

Introduction

Hydrogen is a promising alternative as an energy carrier since it can be clean, efficient and derived from diverse resources including renewables (biomass, wind, solar, geothermal), fossil fuels and nuclear energy [1]. For its worldwide use, developments in the production, storage, transportation and application of hydrogen must be achieved. In the area of hydrogen storage, numerous studies have been conducted with the aim of developing low cost, safe and efficient materials based on a wide variety of materials, including metal or complex hydrides [2]. The Mg-based Mg_2TH_x ternary hydrides (T = Fe, Co and Ni transition metals) stand out because of their high gravimetric (5.5, 4.5 and 3.6 wt.%) and volumetric (150, 125 and 97 g/L) hydrogen capacities for Mg_2FeH_6, Mg_2CoH_5 and Mg_2NiH_4, respectively [3]. However, the conventional synthesis of these phases by hydrogenation is not trivial, since the compounds Mg_2Fe and Mg_2Co, which could be used as precursors for hydrogen treatments, do not exist in the corresponding equilibrium phase diagrams.

The synthesis, structure and properties of the Mg_2CoH_5 complex hydride were firstly reported by Zolliker et al. [4]. At room temperature the β-Mg_2CoH_5 has a tetragonal crystalline structure with space group P4/nmm (a = 0.4480 nm and c = 0.6619 nm) presenting square-pyramidal CoH_5^{4-} ions. The authors were also the first to report the phase transition at 215 °C from the low temperature β-Mg_2CoH_5 to the high temperature γ-Mg_2CoH_5, which has a body-centered cubic structure with space group Fm3m (a = 0.6453 nm for the deuteride Mg_2CoD_5), where the H atoms are distributed on the 24e Wyckoff positions (x, 0, 0) with x = 0.2368 and occupancy of 0.86.

The initial approach used by investigators to synthesize Mg_2CoH_5 was to sinter 2 Mg-Co mixtures under high hydrogen pressures (4–9 MPa) at high temperatures (400–450 °C) for long times (1–10 days). However, such severe processing conditions resulted in reaction yields lower than 30% [4–6]. Chen et al. [7] were the first to report the synthesis of Mg_2CoH_5 by reactive milling (RM). Practically complete reaction was achieved by milling MgH_2–Co mixture under 0.1 MPa of H_2 for only 10 h. However, MgH_2 is an expensive product to be used as raw material, since its synthesis is not trivial and involves sintering at high temperature and high H_2 pressures for several days. The complete reaction of the Mg_2CoH_5 by RM using metallic Mg and Co as reactants was not reported. Up to now, the highest yield achieved was 81% through the RM of 2 Mg–Co mixtures under 7.5 MPa of H_2 for 12 h, as reported by Zhang et al. [8]. By measuring the evolution during the hydrogen uptake as a function of milling time, the authors also described the reaction path during the RM synthesis, showing that the reaction occurs in two steps, as follows:

$$2Mg(s) + Co(s) + \frac{5}{2}H_2(g) \rightarrow 2MgH_2(s) + Co(s)$$

$$+ \frac{1}{2}H_2\ (g) \rightarrow Mg_2CoH_5\ \ (s)$$

In the present work the Mg_2CoH_5 was synthesized by RM with a high yield, about 97%, using elemental Co and Mg as reactants. Our research group has already reported the attainment of the Mg_2FeH_6 by RM also with high yields (94%) [9–13]. We have shown previously that the most important parameters for the Mg_2FeH_6 synthesis are related to the intensity of milling, i.e., the transfer rate of mechanical energy from the milling tools to the reactant materials [14,15]. This implies that processing parameters such as type of mill, rotational speed, ball-to-powder weight ratio and hydrogen pressure are all important in defining the formation yield of the complex hydrides.

In addition to examining the synthesis of this phase, the thermal behavior and H-sorption kinetics of the Mg_2CoH_5 phase will be presented. Furthermore, by using in-situ synchrotron XRD coupled with QMS, it will be shown that during the heating of the Mg_2CoH_5 two different hydrogen releasing mechanisms take place. These mechanisms have an important influence on the kinetics of hydrogen desorption. Finally, details concerning the β-Mg_2CoH_5 to γ-Mg_2CoH_5 phase transition and its influence on the complex hydride properties are addressed.

Experimental

Magnesium chips (Aldrich Chemical, 98%, <0.85 mm) and cobalt powder (Aldrich Chemical, 99.9%, <150 μm) were used to prepare 2 Mg + Co mixtures. The metallic elements were weighted and sealed inside a stainless steel milling vial (volume of 250 cm^3) with 25 stainless steel balls (15 with 8 mm and 10 with 10 mm diameter). The ball-to-powder weight ratio was fixed at 40:1. After five cleaning cycles consisting of evacuation and argon backfilling, the milling vial was filled with 30 bar of H_2 (99.999%). A Fritsch P6 planetary mill was used with a rotating speed of 600 rpm. The materials were ball milled for periods ranging from 3 to 24 h at room temperature. No H_2 recharging was required during the milling intervals and the milling experiments were not interrupted for sampling. The reactively-milled powders were manipulated inside an MBRAUM glovebox under a protective argon atmosphere. The glovebox workstation was equipped with a gas purification system that maintained H_2O and O_2 levels below 0.1 ppm.

X-ray diffraction (XRD) was performed using a Rigaku diffractometer equipped with a Cu tube and a graphite monochromator operating at 40 kV and 40 mA. The microstructure was examined by scanning electron microscopy (SEM) using a field emission gun Phillips XL 30 microscope and also by transmission electron microscopy (TEM) using a field emission gun FEI Tecnai G2F20 microscope. Simultaneous differential scanning calorimetry (DSC) and thermogravimetry (TGA) were carried out in a Netzsch STA 449C instrument in order to evaluate the hydrogen desorption behavior of the samples during heating. The gases released during the thermal analyses were detected and identified using a quadrupole mass spectrometer (QMS) coupled to the thermal analysis instrument. The measurements were performed under constant argon flow by heating the sample from room temperature up to 500 °C at 10 °C/min. The kinetics of hydrogen absorption and desorption were measured using a homemade Sieverts apparatus. In this case, the samples were initially heated up to the selected temperatures (300 and 350 °C), and after complete hydrogen desorption, the absorption/

desorption kinetics were measured under 20 and 0.3 bar of H_2, respectively.

In-situ synchrotron radiation powder XRD was performed at the Brazilian Synchrotron Light Laboratory (LNLS) in Campinas-SP at XDS beamline (http://lnls.cnpem.br/beamlines/xrd/xds/) installed in an insertion device section of the ring that have a 4T Superconducting Wiggler given higher photon flux in the 10–30 keV spectral range. The selected X-ray wavelength of 0.0652548 nm (19 keV) and a array of 06 Mythen detectors for data collection allow us to follow the in situ thermal treatment. The sample was encapsulated in quartz capillary tube, which was mounted onto a sample holder coupled with a small resistance furnace, as described in Ref. [16]. To keep the atmosphere inert and to remove the gases released from the sample, the analyses were performed under constant helium flow. In order to detect the gas released from the sample a QMS was coupled to the system. The measurements were carried out in a temperature range from 25 to 550 °C with a constant heating rate of 5 °C/min and the diffraction patterns were collected every 3 min. The lattice parameters of the phases described here were obtained by the Rietveld method through the X'Pert HighScore Plus software. The electron diffraction patterns of the β-Mg_2CoH_5 and γ-Mg_2CoH_5 were simulated by using the JEMS software.

Results

Mg_2CoH_5 synthesis

Fig. 1 shows the XRD patterns of the 2 Mg–Co mixture prepared by RM under H_2 pressure for 3, 6, 12 and 24 h. The XRD pattern from the sample milled for 3 h shows the presence of MgH_2 and Co phases. Mg peaks are barely visible in the XRD pattern indicating that nearly all of the Mg reacted with H_2 during the first 3 h of the RM. The diffraction peaks of β-Mg_2CoH_5 phase were identified in the XRD pattern of the sample ball milled for 6 h while the diffraction peaks of β-MgH_2 and Co had practically disappeared. The sample milled for 12 h appears to contain only the complex hydride as majority phase. No further changes occurred after milling longer than 12 h (compare the XRD pattern of the samples ball milled for 12 and 24 h). One can see that in all XRD patterns in Fig. 1, the diffraction peaks are broad, due to the internal strain and small crystallite sizes induced by ball milling. The reactively-milled powders were analyzed by SEM and the images of the 6 h and 12 h samples are presented in Fig. 2. The 12 h sample predominantly consists of particles with sizes smaller than 1 μm, whereas the 6 h sample is coarser and consists of a mixture of large particles, about 2 μm, with finer ones, these differences in the particles sizes can change considerably the H-sorption behavior of the hydride [17]. The fine particle sizes observed here are due to the use of high-energy conditions that favor the breaking and mixing of the particles, generating a more intimate mixture, which, consequently, should favor the reaction among the metallic elements during RM.

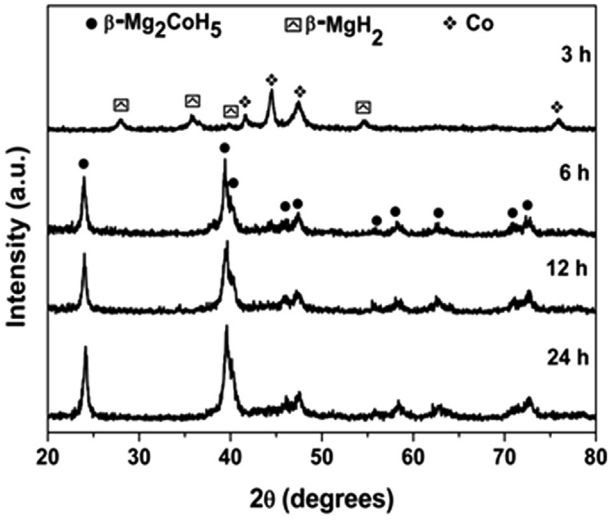

Fig. 1 – XRD patterns of the 2 Mg + Co mixtures processed for 3, 6, 12 and 24 h by RM. (CuKα_1 radiation).

The microstructure of the sample milled for 12 h was examined in greater detail using TEM (Fig. 3). The selected area diffraction pattern (SADP) of the polycrystalline region (Fig. 3(c)) clearly shows that all of the diffraction rings can be indexed according to the tetragonal (P4/nmm) β-Mg_2CoH_5 phase consistent with the XRD results. The bright and dark field image (Fig. 3(a) and (b)) are consistent and indicate that the powders are nanocrystalline – it can be seen that the microstructure of one single powder particle is in fact composed by crystallites in the 10–15 nm range. Therefore, it is demonstrated that RM with an appropriate selection of milling parameters is an effective process for both the synthesis of the complex hydride and in the refinement of the microstructure to the nanoscale.

Thermal analyses and H-sorption kinetics

DSC and QMS curves showing the hydrogen evolution during the heating of the milled samples are shown in Fig. 4. Significantly, the curves from the 3 h sample, which is composed by a mixture of MgH_2 and free Co, and those from the 6 h sample, composed only by the β-Mg_2CoH_5 phase, contain only a single endothermic peak. On the other hand, the curves from the 12 h and 24 h samples, which are composed only of the β-Mg_2CoH_5 phase, contain two well-distinguished endothermic peaks, Fig. 4(a). By analyzing the QMS curves, Fig. 4(b), one can see that all endothermic peaks are associated with hydrogen release from the samples. Although the 6 h and 12 h samples present practically only β-Mg_2CoH_5 as majority phase (Fig. 1), both present different desorption behavior, as can be seen by thermal analyses results (Fig. 4), showing that the microstructural refinement promoted by the additional milling time in the 12 h sample (Fig. 2) plays an important role in the H-desorption properties of the complex hydride. In Section Hydrogen releasing mechanisms, it will be shown that these two endothermic peaks are in fact related to two different mechanisms of hydrogen release. In all cases, a relatively low onset desorption temperature was observed – although it increased with increasing milling time – starting at ~212 °C for the 3 h sample compared with a reported value of 348 °C for nanocrystalline MgH_2 [13]. This result suggests that Co improves the hydrogen desorption kinetics of MgH_2, as already

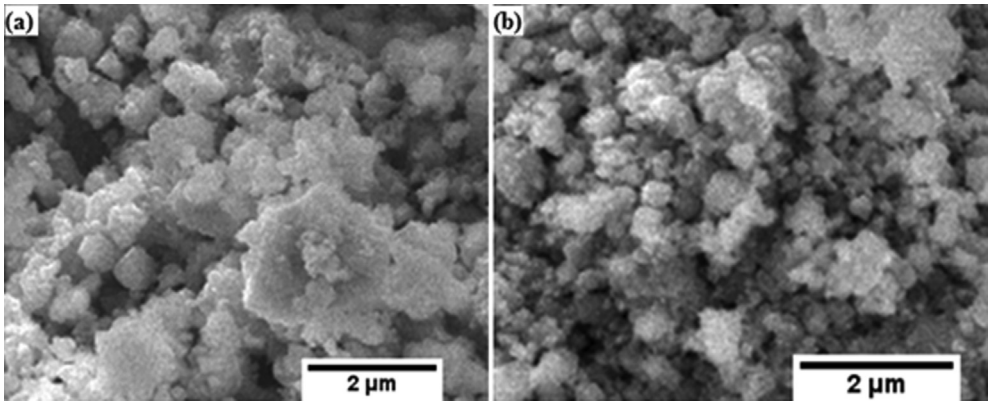

Fig. 2 – SEM images using the secondary electron (SE) mode of the 2 Mg + Co mixtures milled for (a) 6 h and (b) 12 h.

well-established for other transition metal additions to MgH_2 [18]. The onset temperatures of desorption of the 6 h, 12 h and 24 h samples were also relatively low, ranging from 220 to 238 °C. The 12 h and 24 h samples that were rich in Mg_2CoH_5 also exhibited exothermic peaks at higher temperatures, i.e., above 400 °C. As already reported, these peaks may be related to the formation of Mg–Co intermetallics, such as MgCo and $MgCo_2$, after hydride decomposition [19,20]. The second interesting observation is the absence of the endothermic peak close to 200 °C related to the allotropic phase transition of the Mg_2CoH_5. The absence of such peaks in the DSC curves will be discussed further in Section On the β to γ phase transition.

Thermogravimetric analysis was performed on the 12 h sample (Fig. 5) and, as can be seen, the weight loss of the sample was 4.35%, which is close to the theoretical gravimetric capacity of Mg_2CoH_5 (4.48 wt.%). This indicates a reaction yield of approximately 97%. This is the first work to report the synthesis of the Mg_2CoH_5 by RM from the metallic elements as reactants with almost complete reaction. The kinetics of hydrogen absorption and desorption of the 12 h sample at 300 and 350 °C was evaluated and the results are presented in Fig. 6. It can be observed that increasing the temperature results in higher hydrogen capacity and faster kinetics. For hydrogen absorption, after only 30 min, the theoretical capacity of the Mg_2CoH_5 was achieved at 350 °C. On

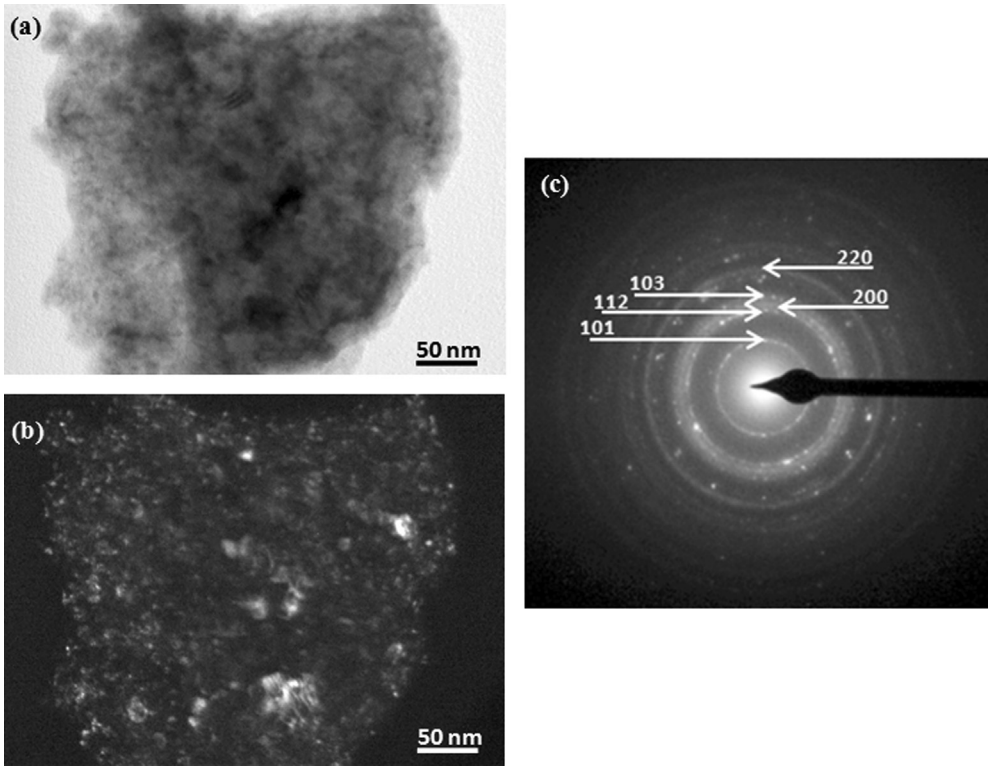

Fig. 3 – TEM images of the 12 h milled sample. (a) Bright field, (b) Dark field (using 112 and 200 rings) and (c) SADP showing the reflections from β-Mg_2CoH_5.

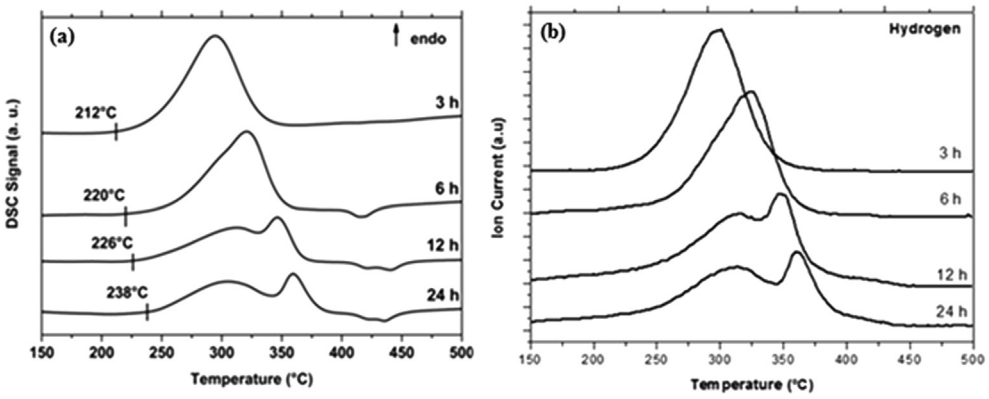

Fig. 4 – Simultaneous DSC (a) and QMS (b) analyses of the 2 Mg + Co mixtures processed for 3, 6, 12 and 24 h by RM under H_2 pressure. Heating rate: 10 °C/min.

the other hand, considerably lower hydrogen absorption rates were observed at 300 °C, Fig. 6(a). In the case of desorption, the effect of the temperature is even more pronounced, Fig. 6(b). At 350 °C, the hydrogen is fully released after only 100 s while at 300 °C more than 40 min are necessary for complete desorption of the Mg_2CoH_5. This significant change in the H-desorption kinetics by increasing only 50 °C is in fact related to two hydrogen releasing mechanisms that take place when the Mg_2CoH_5 is heated, as it will be demonstrated in the Section Hydrogen releasing mechanisms.

Hydrogen releasing mechanisms

Fig. 7(a) shows the results of the in-situ synchrotron XRD experiments carried out on the 12 h sample. It can be seen that at room temperature only the β-Mg_2CoH_5 phase is observed, in agreement with Fig. 1. Even with the absence of the endothermic peak in the DSC curve, Fig. 4(a), through the in-situ XRD analysis it is clear that the β-Mg_2CoH_5 to γ-Mg_2CoH_5 phase transition occurs between 185 and 205 °C. The decomposition of the γ-Mg_2CoH_5 structure starts at temperatures above 325 °C. At 385 °C, practically all of the γ-Mg_2CoH_5 had decomposed into Mg and Co. The Mg–Co intermetallic compounds starts to appear at temperatures close to 400 °C. In spite of the different heating rate employed, the results are in good agreement with the exothermic peaks observed in the DSC curves, and are similar to those reported by Norek et al. a few years ago [20]. In this paper, the authors state that at temperatures close to 350 °C, the γ-Mg_2CoH_5 decomposes directly into Mg and Co, similar to what is seen in Fig. 7(a). However, by examination of the QMS results, carried out simultaneously to the in-situ XRD, Fig. 7(b), it can be seen that a considerable amount of hydrogen is released from the sample before the decomposition of the γ-Mg_2CoH_5 structure. Small amounts of hydrogen are already released from the sample between 100 and 200 °C, but at 200 °C, just after the β to γ phase transition, the detection of released hydrogen increases considerably up to 320 °C. At this temperature, the γ-Mg_2CoH_5 structure starts to decompose into Mg and Co, and a new change in the detection of the released hydrogen is observed. With both complementary analyses, it can be clearly observed that, in fact, two different hydrogen release mechanisms take place when the sample is heated. At low temperatures ranging from 200 to 320 °C, a significant amount of hydrogen is released from the sample with no change in the crystalline structure of the γ-Mg_2CoH_5 complex hydride. This hydrogen releasing mechanism can be described by the following equation:

$$\gamma - Mg_2CoH_5(s) \rightarrow \gamma - Mg_2CoH_x(g) + \frac{(5-x)}{2}H_2(g)$$

At 320 °C, the hydride structure becomes unstable and starts to decompose into Mg and Co, resulting in a second mechanism of hydrogen release:

$$\gamma - Mg_2CoH_x(s) \rightarrow Mg(s) + Co(s) + \frac{(x)}{2}H_2(g)$$

In addition to the in-situ XRD and the mass spectrometry analyses, the onset temperatures of the double endothermic peaks in the DSC curve of the 12 h sample, Fig. 4(a), also corroborates strongly with the two mechanisms proposed. These two different hydrogen desorption mechanisms of the Mg_2CoH_5 are being proposed here for the first time.

On the β to γ phase transition

The existence of the β-Mg_2CoH_5 to γ-Mg_2CoH_5 phase transition and their respective structures were first reported by Zolliker et al., in 1984 [4]. Table 1 and Fig. 8(a) and (b) present the β-Mg_2CoH_5 and γ-Mg_2CoH_5 structures. The low temperature β-Mg_2CoH_5 has a tetragonal structure with the P4/nmm space group and with Mg atoms in the Wyckoff 2a and 2b sites and Co atoms in the Wyckoff 2c (1/4,1/4,0.2561) sites (octahedral centers). The H atoms surround the Co atoms in an ordered square-pyramidal configuration in 2c (1/4, 1/4, 0.4972) and 8j (0.4879, 0.4879, 0.2257) Wyckoff sites. As reported by Zolliker et al. [4], at 215 °C (upon heating) the low symmetry β-Mg_2CoH_5 transforms to the cubic γ-Mg_2CoH_5 phase which has the Fm3m space group, with Mg atoms in the 8c Wyckoff sites, Co in the 4a Wyckoff sites and H randomly distributed in an octahedral arrangement around each Co atom in the 24e Wyckoff sites. Zolliker et al. [4] also reported that the H occupancy is ~0.86, which closely agrees with the expected

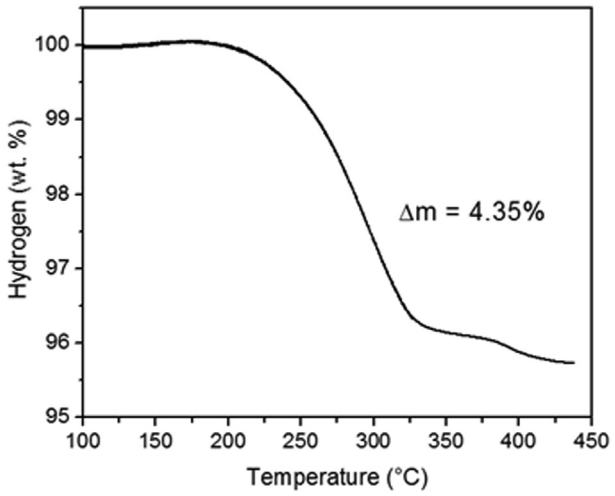

Fig. 5 – Thermogravimetric analysis of the sample milled for 12 h.

occupancy of 5/6 needed to yield the Mg_2CoH_5 stoichiometry. The lattice parameters of both phases are also presented in Table 1. It can be seen that the ratio a_γ/c_β is ~1 and a_γ/a_β is ~$\sqrt{2}$. It is suggested that the β-Mg_2CoH_5 to γ-Mg_2CoH_5 phase transition must be displacive since it appears to occur with no release of hydrogen. Since displacive phase transitions involve relatively subtle changes in the crystal structure, the resulting orientation relationship between both phases is well defined. As suggested by the fact that a_γ/c_β ~1 and a_γ/a_β~$\sqrt{2}$, and as can be seen in Fig. 8(c), the $[001]_\beta$ is expected to lie parallel to the $[001]_\gamma$ and the $[110]_\beta$ parallel to $[100]_\gamma$ or $[010]_\gamma$. These relationships can be more clearly seen by observing the simulated electron diffraction pattern (EDP) of the β-Mg_2CoH_5 structure along the [110] zone axis and along the [100] zone axis of the γ-Mg_2CoH_5 structure (Fig. 9). As these zone axes are parallel, the EDP of both structures must be similar. One can see that the {00l} reflections, black arrows, are the same for both EDPs, however, the {220} reflections of the β-Mg_2CoH_5 become the {040} reflections of the γ-Mg_2CoH_5, red arrows. As the γ-Mg_2CoH_5 has a higher symmetry structure, fewer reflections are seen in the EDP as a result of the disappearance of the mixed h, k, l reflections for the general reflection conditions of the Fm3m space group (h, k, l: h + k, h + l, k + l = 2n).

Thus, it can be confirmed that both structures have the following orientation relationships:

β[001]//γ[001]and β(001)≡γ(001)

β[110]//γ[010] and β(110)≡γ(020)

Based on these orientation relationships and the similar nature of these structures, it is anticipated that the phase transition between β-Mg_2CoH_5 and γ-Mg_2CoH_5 takes place by small displacements along the main axes of the β-Mg_2CoH_5 phase. In order to estimate the magnitude of such displacements, the lattice parameters for both structures at several temperatures were calculated by the Rietveld method using the in-situ XRD data presented in Fig. 7(a). Fig. 10 shows examples of the Rietveld analyses carried out in the β-Mg_2CoH_5 phase at 65 °C, Fig. 10(a) and (c), and in the γ-Mg_2CoH_5 at 205 °C, Fig. 10(b) and (d). All analyses were performed as shown in these examples, in efforts to obtain the best fitting possible between the calculated peak positions and the experimental data. The results of the lattice parameters of the β-Mg_2CoH_5 and γ-Mg_2CoH_5 as a function of temperature are presented in Fig. 11(a)–(c). As can be seen, the lattice parameters of both phases increase slightly with increasing temperature due to thermal expansion. By extrapolation of the linear fits shown in Fig. 10(a) and (b) to room temperature we find a = 0.4527 nm and c = 0.6673 nm, slightly higher than the lattice parameters presented in Table 1 for the β-Mg_2CoH_5 as determined by Zolliker et al. [4]. Such differences can be resulted from small deviations in the experimental measurements; however, as all XRD data are affected by these deviations, a good estimation of the displacements that occur during the phase transition can be performed with these results. By using the linear fitting presented in Figure (a), (b) and (c) it is possible to calculate the interplanar spacing of the equivalent planes previously described for the β-Mg_2CoH_5 and γ-Mg_2CoH_5phases. For example, at 215 °C, the following values are derived from the experimental data:

$$d_{\beta 110} = 0.3231\ \text{nm} \rightarrow d_{\gamma 020} = 0.3272\ \text{nm}$$

and

$$d_{\beta 001} = 0.6696\ \text{nm} \rightarrow d_{\gamma 001} = 0.6544\ \text{nm}$$

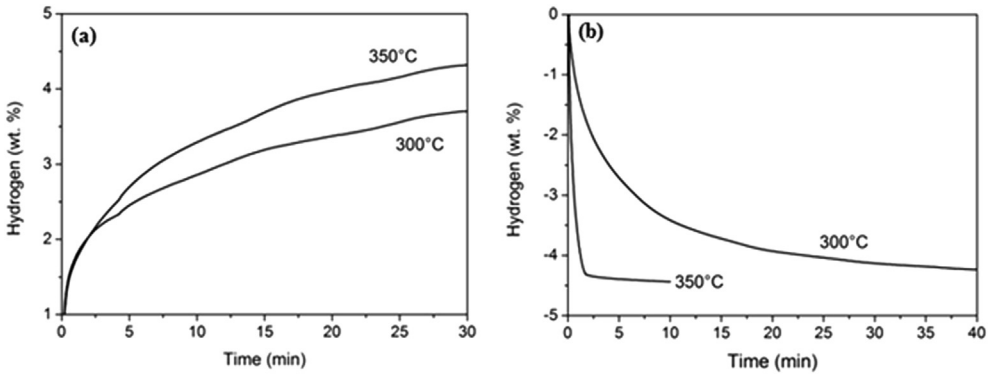

Fig. 6 – Hydrogen absorption (a) and desorption (b) kinetics curves at 300 °C and 350 °C for the 12 h sample. The hydrogen absorption and desorption were measured under 20 bar and 0.3 bar, respectively.

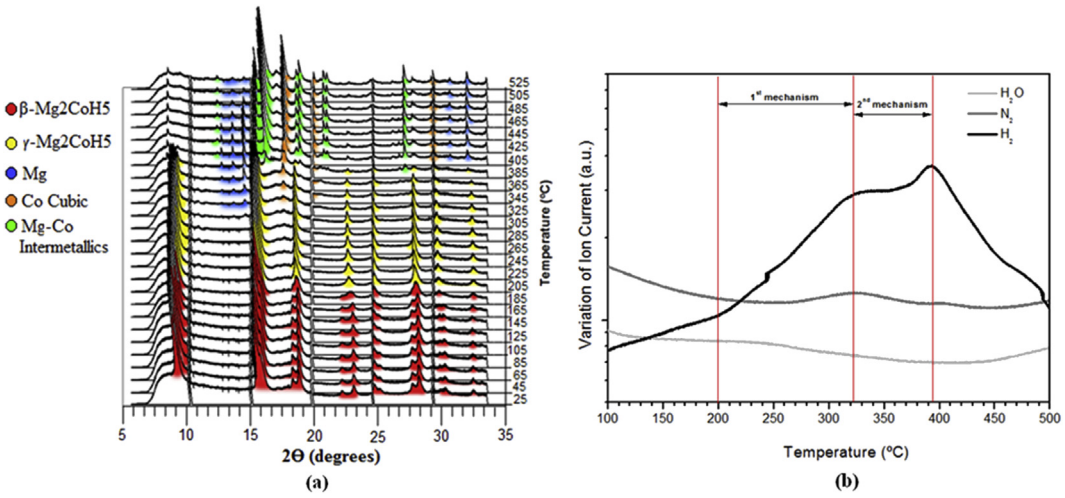

Fig. 7 – (a) In-situ XRD analyses of the 12 h milled sample from room temperature to 525 °C ($\lambda = 0.0653$ nm). (b) QMS analysis coupled to the in-situ XRD analysis showing the hydrogen releasing during the heating. Heating rate: 5 °C/min.

Thus, it appears that at 215 °C the β-Mg_2CoH_5 to γ-Mg_2CoH_5 phase transition takes place by a small elongation of the a and b axes, which results in an elongation of 0.0041 nm (about 1.26%) in the β[110] direction, and by a contraction of 0.0151 nm (about 2.25%) along the β[001] direction or c axis. Thus, it is clear that both structures have well-determined orientation relationships and that the phase transition occurs by subtle displacements of the unit cell. The volume of the unit cell for both phases divided by the number of Mg_2CoH_5 formula units as a function of temperature were also calculated, Fig. 11(d). As can be seen the β-Mg_2CoH_5 to γ-Mg_2CoH_5 phase transition is accompanied by a very small increase in the volume per formula unit. At 215 °C the volume increases of 0.000183 nm^3/Mg_2CoH_5 formula unit, around 0.26%. This result shows that the increase in the volume of the unit cell after the phase transition is insufficient and does not correlate with hydrogen release from the structure.

Fig. 12 presents a region of the in-situ XRD of the 12 h milled sample showing in greater detail the β-Mg_2CoH_5 to γ-Mg_2CoH_5 phase transition. As can be clearly seen, the phase transition starts to take place just above 180 °C when the double reflection characteristics of the tetragonal phase start to become asymmetric and broad due to the coexistence of the single peaks of the cubic phase. In addition, it can be seen that both phases coexist over approximately 20 °C, and, above 200 °C, only the γ-Mg_2CoH_5 phase exists. Although the phase transition be clearly seen through the in-situ XRD analyses, no endothermic peaks related to this transformation is observed in the DSC curve of the 12 h milled sample presented in Fig. 4, as reported before, see for example [20].

In order to understand the reason for the absence of such endothermic peak, the 12 h milled sample was subjected to thermal cycling from room temperature up to 230 °C using the DSC furnace (Fig. 13). During the first heating cycle, no peak is seen in the DSC curve, but when the sample is heated again, well-defined endothermic peaks at 219 °C and 223 °C are observed during the second and third cycles, respectively. These peaks must be related to the β-Mg_2CoH_5 to γ-Mg_2CoH_5 phase transition. Based on these results, it is concluded that the endothermic peak was not observed in the first heating of the sample because the high energy stored in the material resulting from the high energy mechanical milling (high density of defects, interfaces and microstresses) is sufficient to promote the β-Mg_2CoH_5 to γ-Mg_2CoH_5 phase transition and, consequently, no substantial energy must be transferred from the surroundings, resulting in no changes in the DSC curve. This also can explain why the transition temperature of the as-milled sample is lower than those usually reported in the literature. After the first thermal cycle, as the stored energy was already dissipated, when the sample is heated again the

Table 1 – β-Mg_2CoH_5 and γ-Mg_2CoH_5 structures [4].

β-Mg_2CoH_5 at 25 °C			γ-Mg_2CoH_5 at 225 °C		
Space group	P4/nmm	(N° 129)	Space group	Fm3m	(N° 225)
Cell parameters (nm)	$a = 0.4480$	$c = 0.6619$	Cell parameters (nm)	$a = 0.6453$	
Positions			Positions		
Mg (1)	2a	(¾, ¼, 0)	Co	4a	(0,0,0)
Mg (2)	2b	(¾, ¼, ½)	Mg	8c	(¼, ¼, ¼)
Co	2c	(¼, ¼, 0.2561)	H	24e	(0, 0, 0.2348)
H (1)	2c	(¼, ¼, 0.4972)	Occupancy = 0.86		
H (2)	8j	(0.4879, 0.4879, 0.2257)			

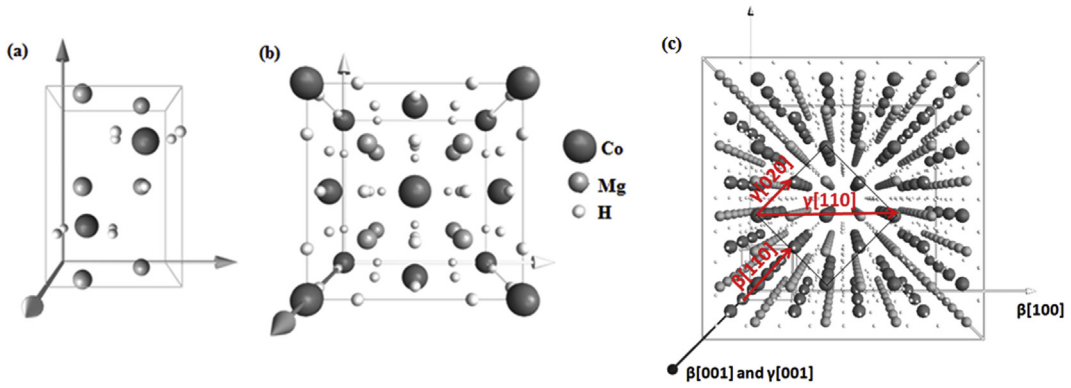

Fig. 8 – Schematic structure of (a) β-Mg_2CoH_5 (b) γ-Mg_2CoH_5 and (c) expanded 4 × 4 × 4 β-Mg_2CoH_5 unit cells showing relationship between both structures: β[001]//γ[001] and β[100]//γ[020].

phase transition takes place at higher temperatures and this is accompanied by an endothermic DSC peak.

Discussion

In this study, it has been shown that the Mg_2CoH_5 complex hydride can be synthesized with very high yields using RM of the metallic elements in a hydrogen atmosphere. In only three hours, practically all the metallic Mg reacts to form MgH_2, which agrees with the reaction path during the RM synthesis of the complex hydrides reported by Zhang et al. [8]. After 12 h of RM, a complete reaction between the magnesium hydride and the metallic cobalt is achieved resulting in a very fine powder of almost 100% Mg_2CoH_5 with nanocrystalline structure. The rapid and practically full synthesis of Mg_2CoH_5 by RM from the metallic elements is attributed to an appropriate choice of milling parameters. As reported by Leiva et al. [12,13], a high yield synthesis of the complex hydride Mg_2FeH_6, which belongs to the same complex hydride family as Mg_2CoH_5, requires high energy transfer rates during ball milling. The results obtained for Mg_2FeH_6 [12,13] and Mg_2CoH_5 (this study) are supported by the model proposed by Bab and Mendoza-Zélis [14,15] for hydride formation kinetics during RM. Specifically, they proposed a quantitative model for the extent of reaction based on an analogy between the mechanical energy during milling and the thermal energy in thermally-activated processes, i.e., they consider that the energy transferred to the material during mechanical processing plays a similar role as other forms of energy usually employed to induce physical or chemical transformations. These studies have shown that the same extent of reaction is reached when the same amount of energy is transferred to a unit mass of material (same specific energy dose). It is worth pointing out that this is the first time in the literature that practically complete reaction to form the Mg_2CoH_5 has been achieved by RM, using as reactants the Mg and Co metallic elements. RM is also very efficient in refining the microstructure of the Mg_2CoH_5 product. It was shown that the 12 h milled sample is composed of very fine powders with particle sizes below 1 μm and crystallite sizes below 15 nm. The increase in the interfacial area due to the microstructural refinement is critical for improving the hydrogen storage properties. This becomes evident when the onset temperature of hydrogen desorption from the reactively mechanical-milled Mg_2CoH_5, occurs between 220 and 238 °C compared with sintered Mg_2CoH_5 in which the H-desorption occurs over the temperature range from 300 to 390 °C [19–21].

The behavior of the Mg_2CoH_5 synthesized by RM during heating was studied using a combination of several techniques such as DSC, QMS, ATG, TEM and in-situ synchrotron XRD. From the in-situ XRD analysis, it is possible to see that, at 180 °C, the β-Mg_2CoH_5 to γ-Mg_2CoH_5 allotropic phase transition initiates by a displacive phase transition where the tetragonal β-Mg_2CoH_5 transforms to the cubic γ-Mg_2CoH_5 by a small contraction of the c axis and by a very small elongation of the a and b axes. Both phases have well defined orientation relationships being the β(001) and γ(001)and the β(110) and γ(020) equivalent planes. Furthermore, this is the first study in the literature to thoroughly describe this Mg_2CoH_5 allotropic phase transition. As pointed out above, when the as-milled Mg_2CoH_5 is subjected to DSC analysis, no endothermic peak related to the allotropic phase transition was observed. However, when the material is subjected to thermal cycles from room temperature up to 230 °C small endothermic peaks at ~220 °C start to appear. It is suggested that the absence of the endothermic peak from the as-milled sample is masked by the large amount of stored energy in the mechanicall-milled material in the form of defects, interfaces, microstresses and strains; this is sufficient to supply the necessary energy to induce the phase transition. This is supported by all the DSC results reported in the literature thus far, see Table 2. We can observe that all DSC curves of the Mg_2CoH_5 synthesized by sintering present the endothermic peak related to the β-Mg_2CoH_5 to γ-Mg_2CoH_5 phase transition, while no peaks related to this phase transition have been reported for the DSC curves from Mg_2CoH_5 synthesized by RM. Fernandez et al. [21] performed DSC analyses of the as-milled Mg_2CoH_5 and after several hydrogen desorption/absorption cycles. No peak can be seen in the DSC curves of the as-milled material. On the other hand, a small endothermic peak at 200 °C related to the allotropic phase transition is clearly seen in the DSC curve of the cycled material [22,23].

Considerable hydrogen release is detected by QMS just after the β to γ phase transition. However, no changes in the in-situ XRD patterns can be observed up to 325 °C. Thus, we propose a

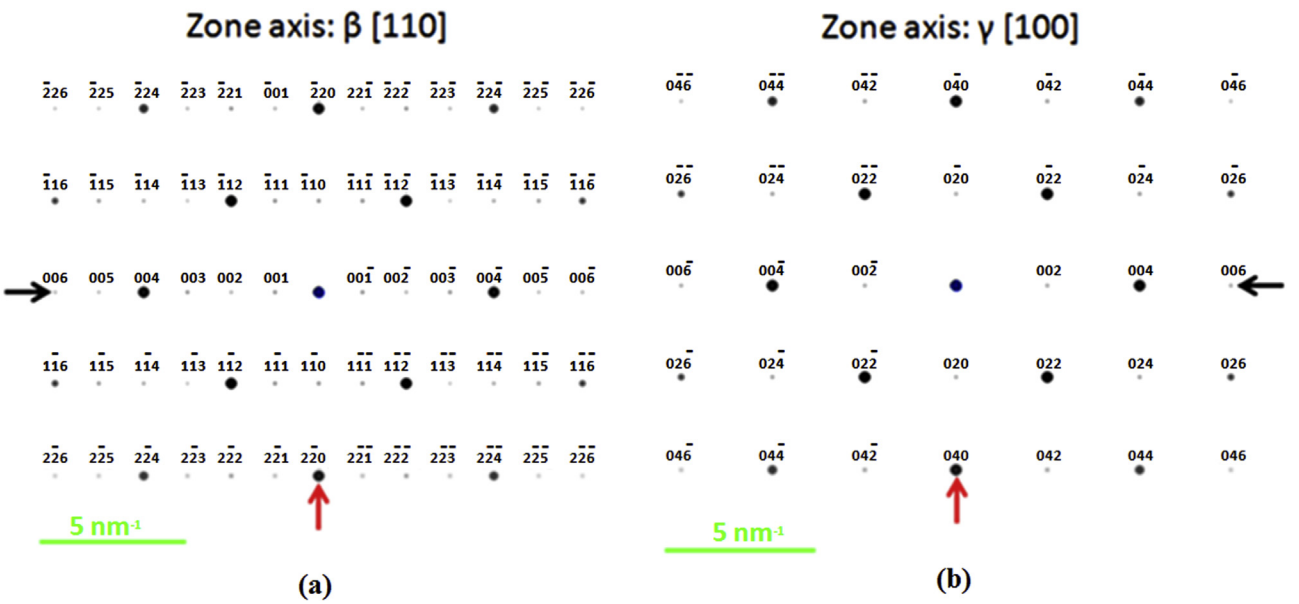

Fig. 9 – Calculated electron diffraction pattern of (a) β-Mg_2CoH_5 and (b) γ-Mg_2CoH_5 structures showing the equivalent planes: β(004)//γ(004), black arrows, and β(−220)//γ(040), red arrows. (For interpretation of the references to colour in this figure legend, the reader is referred to the web version of this article.)

diffusional hydrogen desorption mechanism, in which the H atoms diffuse from their interstitial positions reacting with each other to form H_2. While the hydrogen is released from the sample, the occupancy factor of the Wyckoff 24e sites is reduced resulting in the γ-$Mg_2CoH_{x<5}$ phase, but no changes in the face centered structure occurs and, consequently, no changes in the XRD patterns can be seen. At approximately 325 °C the γ-Mg_2CoH_x starts to be unstable and decomposes into Mg, Co and H_2. Up to 385 °C, all the remaining hydrogen is released from the sample by the hydride decomposition. Both the diffusional and the hydride decomposition mechanisms involved in the hydrogen desorption are supported by the coupled DSC and QMS analyses, Fig. 4(a) and (b). Two well-distinguished endothermic peaks with onset temperatures of 226 and 325 °C are clearly related to the two hydrogen release events. The thermogravimetric analysis presented in Fig. 5 shows that at 300 °C approximately 2.5%wt.of hydrogen (55% of the theoretical capacity) was released from the sample, showing that the diffusional mechanism has a considerable importance in the hydrogen desorption of the Mg_2CoH_5. However, as shown in Table 2, all sintered Mg_2CoH_5 samples present higher onset temperatures of desorption, i.e. 350 °C or above. This clearly indicates that the diffusional mechanism of hydrogen desorption is completely affected by the

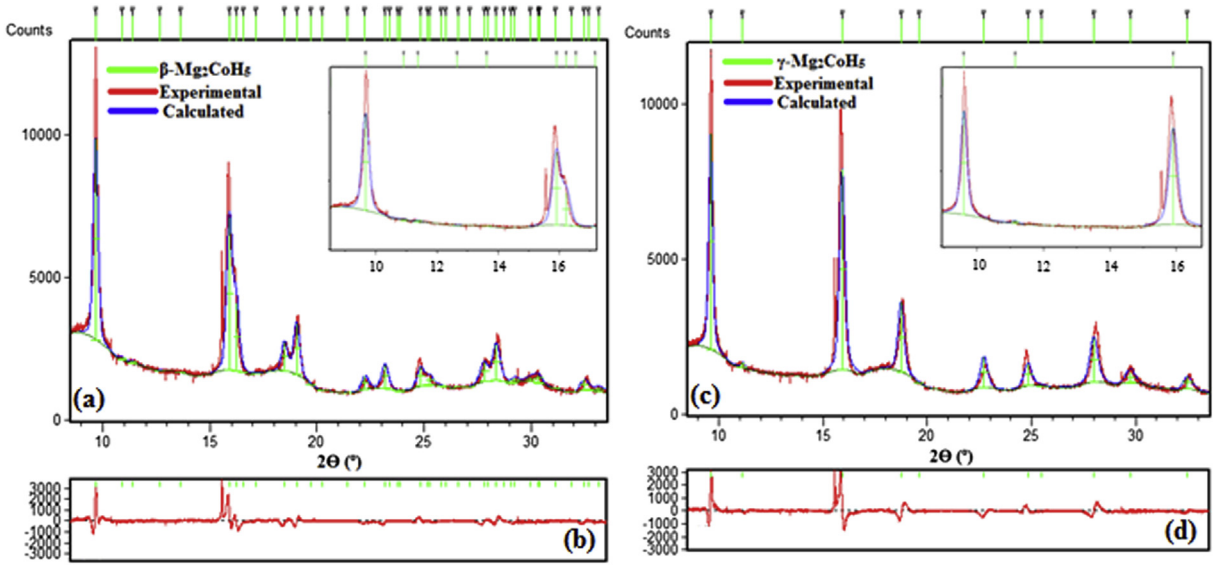

Fig. 10 – Rietveld refinement results of the 12 h milled sample (a) at 65 °C and (b) at 205 °C used to calculate the lattice parameters of β-Mg_2CoH_5 and γ-Mg_2CoH_5, respectively. (c) and (d) the intensity difference between the calculated and experimental curves. ($\lambda = 0.0653$ nm).

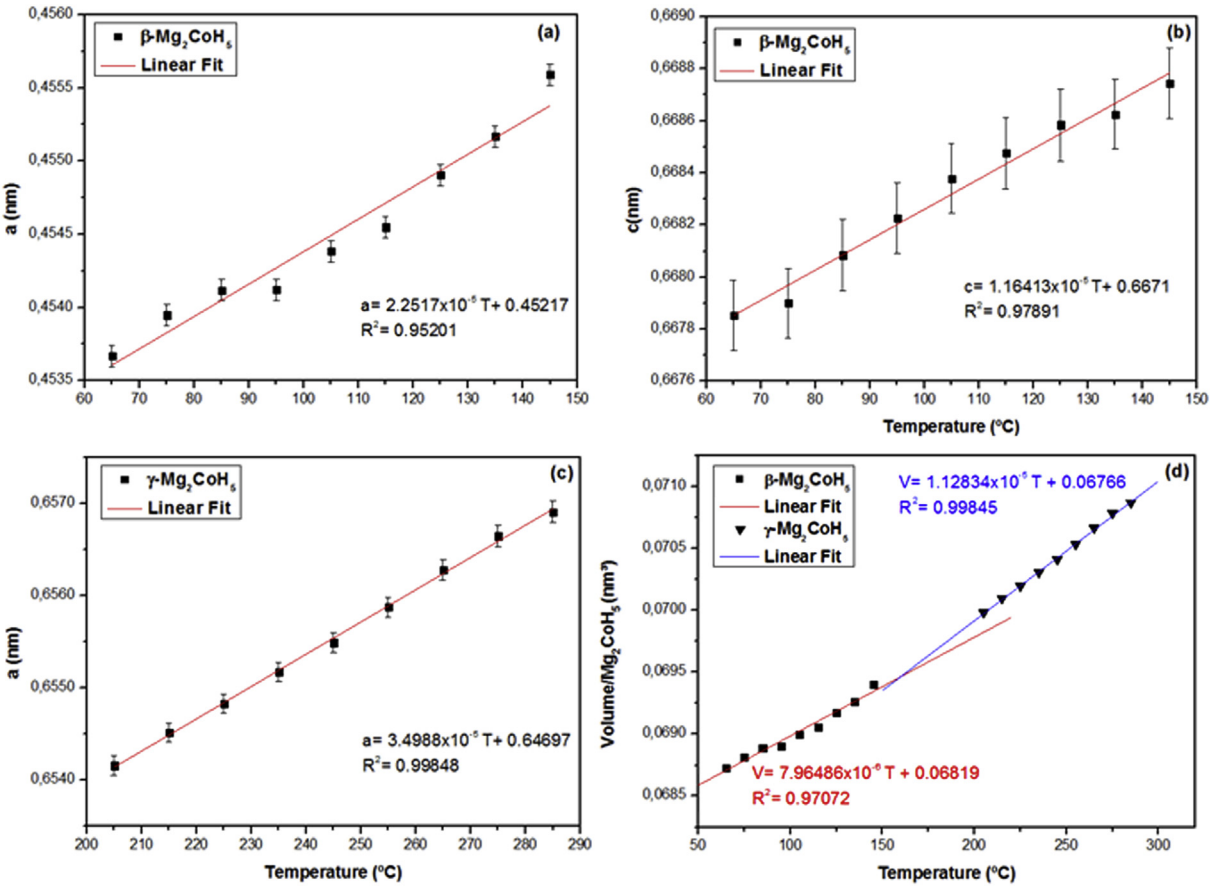

Fig. 11 – Lattice parameters as a function of temperature measured by Rietveld refinement of (a) and (b) β-Mg_2CoH_5; (c) γ-Mg_2CoH_5 and (d) volume per Mg_2CoH_5 formula as function of temperature for both phases.

microstructural characteristics of the Mg_2CoH_5, taking place only in materials with a high density of interfaces such as the reactively-milled complex hydride presented here. As reported by Zaluski, L. et al. [24], the higher surface-to-volume ratio and the elevated fraction of grain boundaries in nanocrystalline materials allow the hydrogen atoms to fill the easily accessible sites at the disordered grain boundaries, avoiding long range diffusion of hydrogen, which results in a higher diffusion coefficient when compared with their correspondent single-crystalline material. This study is the first to report these two different hydrogen release mechanisms for the Mg_2CoH_5 or any other complex hydride.

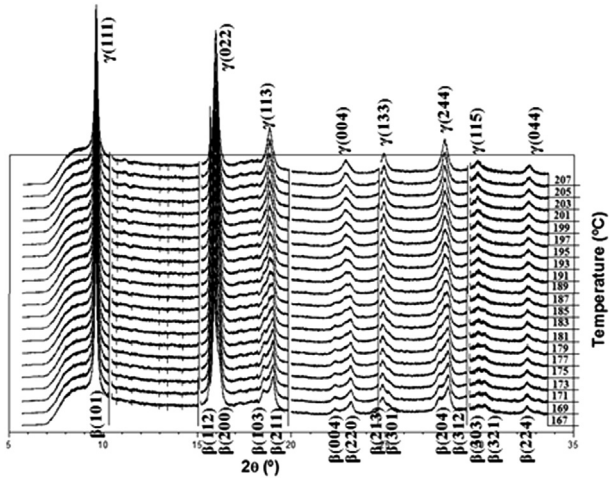

Fig. 12 – In-situ XRD analyses of the 12 h milled sample showing the phase transition from β-Mg_2CoH_5 to γ-Mg_2CoH_5.

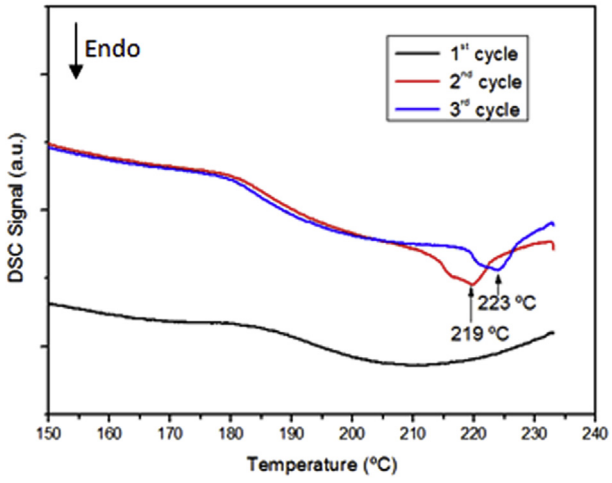

Fig. 13 – DSC heating curves of the 12 h milled sample during the thermal cycling from room temperature up to 230 °C. Heating rate: 10 °C/min.

Table 2 – Summary of the DSC curves of the Mg_2CoH_5 reported in the literature so far.

Synthesis	β to γ phase transition	Onset temperature of desorption	Desorption peak	Ref.
RM	No peak	250 °C	Single peak at 300 °C	[19]
RM	No peak	247 °C	Single peak at 300 °C	[22]
RM	No peak	240 °C	Single peak at 290 °C	[21]
RM + thermal cycling	Small peak at 200 °C	250 °C	Single peak at 300 °C	[21]
Sintering	Small peak at 200 °C	390 °C	Single peak at 400 °C	[21]
Sintering	Small peak at 200 °C	300 °C	Single peak at 350 °C	[20]
Sintering	Small peak at 200 °C	380 °C	Two peaks at 391 and 410 °C	[19]
Sintering	Small peak at 203 °C	390 °C	Single peak at 400 °C	[23]

The H-sorption kinetics curves presented in Fig. 6 shows that the hydrogen absorption/desorption mechanisms have a huge influence in the absorption and desorption kinetics of the Mg_2CoH_5. As demonstrated at 350 °C and atmospheric pressure, the γ-Mg_2CoH_5 is unstable and decomposes into Mg, Co and H_2,which results in very rapid hydrogen desorption kinetics (100 s for complete desorption). On the other hand, at 300 °C and atmospheric pressure, the γ-Mg_2CoH_5 structure is stable, and the hydrogen desorption occurs by a diffusion process, resulting in slower hydrogen desorption kinetics (40 min for complete desorption).

Conclusions

- Nanocrystalline Mg_2CoH_5 was synthesized to very high yields, almost 100%, by high energy reactive mechanical milling.
- The β-Mg_2CoH_5 to γ-Mg_2CoH_5 phase transition occurs by a displacive reaction involving very small displacements of the main axes of the low temperature tetragonal structure. A short elongation of the a and b axes and a contraction in the c axis accompanies this transformation.
- Two different hydrogen desorption mechanisms occur in the milled Mg_2CoH_5. At low temperatures, below 325 °C, the hydrogen release is by a diffusional process with no change in the face centered cubic structure of the γ-Mg_2CoH_5 phase. Above 325 °C, the γ-Mg_2CoH_x becomes unstable and the hydrogen is desorbed from the sample by decomposition of the complex hydride into Mg, Co and H_2.
- The H desorption kinetics are strongly affected by the desorption mechanism, i.e., slower kinetics are associated with the diffusional mechanism and much faster kinetics when the H desorption mechanism is the decomposition of the γ-Mg_2CoH_5 into the metallic elements and H_2.

Acknowledgments

The authors would like to thank the Brazilian institutions FAPESP, CNPq, CAPES and LNLS for the financial support.

REFERENCES

[1] Satyapal S, Petrovic J, Read C, Thomas G, Ordaz G. The US Department of Energy's National Hydrogen Storage Project: progress towards meeting hydrogen-powered vehicle requirements. Catal Today 2007;120:246–56.
[2] Huot J, Ravnsbaek DB, Zhang J, Cuevas F, Latroche M, Jensen TR. Mechanochemical synthesis of hydrogen storage materials. Prog Mater Sci 2013;58:30–75.
[3] Yvon K. Complex transition-metal hydrides. Chimia 1998;52:613–9.
[4] Zolliker P, Yvon K, Fischer P, Schefer J. Dimagnesium cobalt(I) pentahydride, Mg_2CoH_5, containing square-pyramidal CoH_5^{4-} anions. Inorg Chem 1985;24:4177–80.
[5] Huot J, Hayakawa H, Akiba E. Preparation of the hydrides Mg_2FeH_6 and Mg_2CoH_5 by mechanical alloying followed by sintering. J Alloy Compd 1997;248:164–7.
[6] Selvam P, Yvon K. Synthesis of Mg_2FeH_6, Mg_2CoH_5 and Mg_2NiH_4 by High-pressure sintering of the elements. Int J Hydrogen Energ 1991;16:615–7.
[7] Chen J, Takeshita HT, Chartouni D, Kuriyama N, Sakai T. Synthesis and characterization of nanocrystalline Mg_2CoH_5 obtained by mechanical alloying. J Mater Sci 2001;36:5829–34.
[8] Zhang JX, Cuevas F, Zaidi W, Bonnet JP, Aymard L, Bobet JL, et al. Highlighting of a single reaction path during reactive Ball milling of Mg and TM by quantitative H_2 Gas sorption analysis to form ternary complex hydrides (TM = Fe, Co, Ni). J Phys Chem C 2011;115:4971–9.
[9] Asselli AAC, Botta WJ, Huot J. Formation reaction of Mg_2FeH_6: effect of hydrogen Absorption/desorption kinetics. Mater Res-Ibero-Am J 2013;16:1373–8.
[10] Asselli AAC, Jorge AM, Ishikawa TT, Botta WJ. Mg_2FeH_6-based nanocomposites with high capacity of hydrogen storage processed by reactive milling. Mater Res-Ibero-Am J 2012;15:229–35.
[11] Asselli AAC, Leiva DR, Jorge AM, Ishikawa TT, Botta WJ. Synthesis and hydrogen sorption properties of Mg_2FeH_6-MgH_2 nanocomposite prepared by reactive milling. J Alloy Compd 2012;536:S250–4.
[12] Leiva DR, Villela ACD, Paiva-Santos CD, Fruchart D, Miraglia S, Ishikawa TT, et al. High-yield direct synthesis of Mg_2FeH_6 from the elements by reactive milling. Solid State Phenomen 2011;170:259–62.
[13] Leiva DR, Zepon G, Asselli AAC, Fruchart D, Miraglia S, Ishikawa TT, et al. Mechanochemistry and H-sorption properties of Mg_2FeH_6-based nanocomposites. Int J Mater Res 2012;103:1147–54.
[14] Bab MA, Mendoza-Zelis L. A model for the kinetics of mechanically assisted gas-solid reactions. Scr Mater 2004;50:99–104.
[15] Bab MA, Mendoza-Zelis L, Damonte LC. Nanocrystalline HfN produced by mechanical milling: kinetic aspects. Acta Mater 2001;49:4205–13.
[16] Figueroa SJA, Gibson D, Mairs T, Pasternak S, Newton MA, Di Michiel M, et al. Innovative insights in a plug flow microreactor for operando X-ray studies. J Appl Crystallogr 2013;46:1523–7.
[17] Varin RA, Czujko T, Chiu C, Wronski Z. Particle size effects on the desorption properties of nanostructured magnesium

dihydride (MgH_2) synthesized by controlled reactive mechanical milling (CRMM). J Alloy Compd 2006;424:356–64.
[18] Liang G, Huot J, Boily S, Van Neste A, Schulz R. Catalytic effect of transition metals on hydrogen sorption in nanocrystalline ball milled MgH_2-Tm (Tm = Ti, V, Mn, Fe and Ni) systems. J Alloy Compd 1999;292:247–52.
[19] Gennari FC, Castro FJ. Formation, composition and stability of Mg-Co compounds. J Alloy Compd 2005;396:182–92.
[20] Norek M, Nielsen TK, Polanski M, Kunce I, Plocinski T, Jaroszewicz LR, et al. Synthesis and decomposition mechanisms of ternary Mg_2CoH_5 studied using in situ synchrotron X-ray diffraction. Int J Hydrogen Energ 2011;36:10760–70.
[21] Fernandez IG, Meyer GO, Gennari FC. Hydriding/dehydriding behavior of Mg_2CoH_5 produced by reactive mechanical milling. J Alloy Compd 2008;464:111–7.
[22] Fernandez IG, Meyer GO, Gennari FC. Reversible hydrogen storage in Mg_2CoH_5 prepared by a combined milling-sintering procedure. J Alloy Compd 2007;446:106–9.
[23] Veron MG, Condo AM, Gennari FC. Effective synthesis of Mg_2CoH_5 by reactive mechanical milling and its hydrogen sorption behavior after cycling. Int J Hydrogen Energ 2013;38:973–81.
[24] Zaluski L, Zaluska A, Strom Olsen JO. Nanocrystalline metal hydrides. J Alloy Compd 1997;253:70–9.